Interfacial Folding and Membrane Insertion of a Designed Helical Peptide†

Alexey S. Ladokhin‡ and Stephen H. White*

Department of Physiology and Biophysics and Program in Macromolecular Structure, University of California, Irvine, California 92697-4560

Received November 26, 2003; Revised Manuscript Received March 11, 2004

ABSTRACT: Nonconstitutive membrane-active proteins, such as diphtheria toxin, must refold on membrane interfaces in the course of membrane penetration. A useful step in deciphering this process is to understand quantitatively the energetics of interface-mediated insertion of model transmembrane helices. A difficulty is that peptides that are sufficiently hydrophobic to span a lipid bilayer have a strong tendency to aggregate in the aqueous phase. To learn how to control the aqueous and membrane behavior of model peptides, we designed a 31-residue peptide (TMX-3) whose properties are described here. TMX-3 has two important structural features: a proline residue in the hydrophobic core that discourages the formation of highly helical aggregates in solution and two histidine residues that allow control of membrane and solution interactions by means of pH changes. The partitioning of TMX-3 into membranes followed complex kinetics, induced helicity, and shifted the histidine pK_a from 6.8 to ~6. Topology measurements disclosed two general modes of TMX-3 binding: interfacial (IF) at low peptide concentrations and partial transmembrane (TM) insertion at higher concentrations. Both modes were reversible and, consequently, suitable for thermodynamic analysis. The free energies of IF partitioning of TMX-3 with deprotonated (pH 7.6) and protonated histidines (pH 4.5) were estimated by fluorescence titration to be −6.7 and −5.0 kcal/mol, respectively. These results show that histidine titration is likely to be important in the pH-dependent refolding of toxins on membrane interfaces and that the most favored state of TMX-3 under any conditions is the IF folded state, which emphasizes the importance of such states in the spontaneous refolding and insertion of diphtheria and other membrane toxins.

Changing from a water-soluble to a membrane-associated state is an essential feature of membrane penetration by bacterial toxins (*1*−*3*), colicins (*4*−*7*), and annexins (*8*−*10*). Membrane insertion of these proteins requires a refolding process that is poorly understood at the molecular level, but the membrane interfacial (IF)[1] region is expected to play a critical role in the refolding event, as described previously (*11*). Model peptides have proven to be extremely useful for characterizing the energetics of IF partitioning (*12*), the interface-catalyzed secondary structure formation (*13*, *14*), and the nonadditivity of hydrophobic and electrostatic interactions at membrane interfaces (*15*). To gain insights into the processes of pH-induced spontaneous transmembrane insertion that underlie the biological activities of toxins, we have designed a new peptide, TMX-3 (Figure 1), whose properties are described in this paper.

TMX-1 Ac-WNALAAVAAALAAVAAALAAVAASKSKSKSK-Amide

TMX-3 GGWAALAAHAAPALAAALAHAAASRSRSRSR-Amide

FIGURE 1: Amino acid sequences of TMX-1 and TMX-3.

Designing a model peptide that is suitable for experimental exploration of the thermodynamics of membrane insertion is challenging, because it is difficult to achieve the high hydrophobicity necessary for membrane binding and insertion into neutral membranes without aggregation in the aqueous phase. An early designed peptide from our laboratory (*16*), TMX-1 (Figure 1), revealed the principal difficulties. It suffered from strong aggregation in solution, indicated by concentration-dependent CD spectra and blue-shifted tryptophan fluorescence (*16*). Furthermore, broadening of the fluorescence emission band revealed conformational heterogeneity of both the water-soluble and membrane-bound forms. These properties precluded the use of TMX-1 for thermodynamic studies of membrane insertion. Our most pressing task in the redesign of TMX-1 was to discourage the formation of highly helical molecular aggregates, the formation of which had been exacerbated by the inadvertent inclusion of an alanine heptad repeat that produces so-called Ala coils (*17*). Besides removing this feature in subsequent

† This work was supported in part by Grant GM-46823 from the National Institute of General Medical Sciences.

* To whom correspondence should be addressed. Phone: (949) 824-7122. Fax: (949) 824-8540. E-mail: SHWhite@uci.edu.

‡ Permanent address: Institute of Molecular Biology and Genetics, National Academy of Sciences of Ukraine, Kiev 03143, Ukraine.

[1] Abbreviations: FRET, Förster resonance energy transfer; IANBD amide, *N*,*N*′-dimethyl-*N*-(iodoacetyl)-*N*′-(7-nitrobenz-2-oxa-1,3-diazol-4-yl)ethylenediamine; LUV, extruded large unilamellar vesicles 100 nm in diameter; LysoPE, 1-palmitoyl-2-hydroxyl-*sn*-glycero-3-phosphoethanolamine; LysoMC, *N*-(7-hydroxyl-4-methylcoumarin-3-acetyl)-1-palmitoyl-2-hydroxy-*sn*-glycero-3-phosphoethanolamine; NBD, 7-nitrobenz-2-oxa-1,3-diazol-4-yl; NBD-PE, *N*-(7-nitrobenz-2-oxa-1,3-diazol-4-yl)-1-palmitoyl-2-oleoyl-*sn*-glycero-3-phosphoethanolamine; POPC, palmitoyloleoylphosphatidylcholine; POPG, palmitoyloleoylphosphatidylglycerol; OBPC, 1-oleoyl-2-(9,10-dibromostearoyl)-*sn*-glycero-3-phosphocholine; POPG, palmitoyloleoylphosphatidylglycerol; R_i, lipid-to-peptide molar ratio; TMX-1, first-generation membrane-binding peptide (Ac-WNALAAVAAALAAVAAALAAVAASKSKSKSK-amide); TMX-3, membrane-binding peptide used in this study (GGWAALAAHLAPALAAALAHALASRSRSRSR-amide); IF, interfacial; TM, transmembrane.

10.1021/bi0361259 CCC: $27.50
Published on Web 04/24/2004

designs, we also abolished the helical "caps" (*18*, *19*), which were found to be unnecessary for achieving high helicity in the TMX design series.

Like its predecessors, TMX-3 has a hydrophobic core that ensures transmembrane stability, a highly charged C-terminus that ensures vectorial insertion, and a tryptophan residue for use as a spectroscopic probe of topology, binding, and aggregation. Two new features were introduced into the hydrophobic core for management of aggregation in the aqueous phase: a pair of His residues to allow the manipulation of peptide topology by changing pH (*20*) and a central Pro residue to discourage helix formation in solution. The hydrophobicity lost by the inclusion of the His and Pro residues was restored by Ala-to-Leu substitutions. The idea of using a central Pro was borrowed from the bee venom peptide melittin, which exists in solution as an unordered monomer but gains helicity upon interaction with membranes due to coupling of partitioning and folding (*13*, *21*). As opposed to the behavior of simple soluble peptides in solution, we concluded from a study (*13*) of membrane binding properties of native melittin and a diastereomer (*22*) that the tendency of Pro to disrupt helical structures on membrane interfaces is weak.

We show here that our most important design goal was achieved. Namely, TMX-3 could exist as a water-soluble monomer at concentrations sufficiently high for membrane partitioning experiments to be conducted easily. Furthermore, its ability to adopt a transbilayer conformation was similar to that of TMX-1, as revealed by oriented circular dichroism (OCD) (*23*−*25*) and LysoMC topology (*26*) methods. Because membrane association of TMX-3 was found to be an equilibrium process, we were able to carry out a comprehensive thermodynamic characterization of the transfer of TMX-3 from the aqueous to the interfacial form at pH values for which histidines are charged or neutral. This allowed us to estimate the pK_a of His in the membrane interface. Our results demonstrate the importance of IF intermediate states in the process of transmembrane helix insertion, even for a simple model peptide.

MATERIALS AND METHODS

Materials. Lipids were purchased from Avanti Polar Lipids (Alabaster, AL). LysoMC was synthesized and purified as described previously (*26*). TMX-3 was synthesized on PEG-PS PAL using FMOC chemistry with an Applied Biosystems 433A automated peptide synthesizer. The details of synthesis and purification were essentially the same as those described for TMX-1 (*16*). Large unilamellar vesicles 1000 Å in diameter were made by extrusion (*27*, *28*). Generally, a 50 mM phosphate buffer was used, except for pH 4.5 samples, for which a 50 mM acetate buffer was used. For all measurements other than CD, the buffers also contained 1 mM EDTA and 3 mM NaN_3. All measurements were taken at 25 °C, except OCD which was carried out at ambient temperature (∼23 °C).

Circular Dichroism, Oriented Circular Dichroism, and Absorbance Spectroscopy. CD measurements were performed using a Jasco-720 spectropolarimeter (Japan Spectroscopic Co., Tokyo, Japan) by scanning from 260 to 185 nm with 1 nm increments using a sample cuvette with an optical path length of 1 mm. Typically, a peptide concentration of 20 μM was used, and 20−50 scans were averaged. At pH 7.6, the sample for the monomeric and aggregated peptide contained 10 and 60 μM peptide, respectively. Spectra of TMX-3 at pH 5.3 were independent of concentration. Samples for membrane-bound TMX-3 contained either 5 mM POPC or 0.5 mM POPG LUV. The peptide concentration of stock solutions was determined with the UV absorbance of tryptophan using a Cary 300 spectrophotometer (Varian Analytical Instruments, Sugar Land, TX). Oriented CD spectra were measured using oriented multibilayers deposited on a quartz slide according to the procedures of Huang and colleagues (*23*−*25*). The details of sample preparation for OCD were the same as those for TMX-1, which were described previously (*16*). Briefly, TMX-3 was codissolved in methanol with POPC at a molar ratio (R_i) of 200 and added dropwise on a slide, dried, and hydrated to a relative humidity of ∼100%. Spectra were recorded at each of four rotations of 90° around the optical axis, coinciding with the beam and normal to the lipid multilayers, and then averaged. The background signal was determined with the same amount of lipid, without TMX-3.

Fluorescence. Fluorescence was measured using a SLM 8100 steady-state fluorescence spectrometer (Jobin Yvon, Edison, NJ) equipped with double-grating excitation and single-grating emission monochromators. The measurements were taken in 4 mm × 10 mm or 2 mm × 10 mm cuvettes. To minimize scattering artifacts, cuvettes were oriented along the excitation beam for spectral measurements and perpendicular to it for intensity measurements (*10*). Cross orientation of polarizers was used (excitation polarization set to horizontal and emission polarization set to vertical) to minimize the scattering contribution from vesicles and to eliminate spectral polarization effects in monochromator transmittance (*10*). Fluorescence spectra were obtained by averaging 10−50 scans collected over a range of 290−500 nm using 1 nm steps. The excitation wavelength was 270 nm. Excitation and emission slits were never wider than 8 nm. The spectral data used for determining fluorescence maxima and widths were collected with 4 nm emission slits. For kinetic measurements, fluorescence emission at 335 nm was collected and averaged every 10 or 30 s. The mixing was initialized by pipet injection of a few microliters of a 50 mM stock solution of LUV into the peptide solution.

Determination of Peptide Topology in Vesicles. The topology of the peptide's Trp residue in membranes was determined using a novel resonance energy transfer method. This method utilizes the lyso-lipid-linked quencher LysoMC, which has been described in detail previously (*26*). The procedure was modified somewhat to take advantage of the single-sample experimental scheme developed by Ladokhin et al. (*29*). Briefly, the idea of the method is as follows. A *cis* or *trans* location of the probe (Trp in this case) is deduced by comparing fluorescence intensities obtained with the LysoMC quencher distributed either symmetrically in both leaflets of the bilayer or asymmetrically, in the outer leaflet only. Because quenching is more efficient within the leaflet than across the bilayer, the difference in quenching from asymmetric and symmetric distributions of the quencher allows the topology of the fluorophore to be determined.

The asymmetric distribution of quenchers is accomplished by adding LysoMC as a micellar solution to peptide-containing vesicles in two steps, to achieve concentrations

of 0.5% (step 1) and 1.0% (step 2) relative to the total lipid. The fluorescence is measured after each step. A small amount of flip-flop-inducing alamethicin (*26*) is then added to create a symmetric distribution of quenchers (step 3). If the fluorescence intensity after step 3 increases to the level of step 1, the Trp is entirely in the outer leaflet. If the intensity remains at the level of step 2, half of the Trp residues are translocated. If the intensity decreases by the value of the difference between steps 1 and 2, all of the Trp residues are in the inner leaflet.

For this approach to work, the peptide by itself must not induce "flip-flop" of the LysoMC across the bilayer. This possibility is examined in separate experiments by taking advantage of the ability of LysoMC to be quenched by NBD-PE, as described by Wimley and White (*26*). Such control experiments demonstrated that under the conditions used in this study, TMX-3 did not cause substantial lipid flip-flop (data not shown).

Curve Fitting. Emission spectra were corrected for the background and fitted to a log-normal distribution for peak-width analysis of the conformational heterogeneity of the Trp environment (*10*). When $\lambda > \lambda_{max} - \rho\Gamma/(\rho^2 - 1)$

$$I(\lambda) = I_0 \exp\left\{\frac{\ln 2}{\ln^2 \rho}\ln^2\left[1 + \frac{(\lambda - \lambda_{max})(\rho^2 - 1)}{\rho\Gamma}\right]\right\} \quad (1a)$$

while when $\lambda < \lambda_{max} - \rho\Gamma/(\rho^2 - 1)$

$$I(\lambda) = 0 \quad (1b)$$

In these expressions, I_0 is the intensity observed at the wavelength of maximum intensity λ_{max}, Γ the full width of the spectrum at half-maximum intensity, and ρ the parameter of asymmetry of the distribution.

The fluorescence intensity in titration experiments was measured at 335 nm and corrected for scattering using the tryptophan zwitterion model, as described in detail previously (*10*). The data were then normalized to the value obtained in the absence of lipid and fitted to the following binding isotherm (*10*, *30*):

$$I([L]) = 1 + I_\infty \frac{K_x[L]}{[W] + K_x[L]} \quad (2)$$

where K_x is the mole-fraction partition coefficient, I_∞ the fluorescence increase upon complete binding, [L] the lipid concentration, and [W] the molar concentration of water (55.3 M). Origin version 6.0 (MicroCal, Inc., Northampton, MA) and Spectra Calc (Galactic Industries Corp., Salem, NH) were used for the nonlinear least-squares fitting of the data to the equations. Free energies of transfer from water to membrane were calculated from

$$\Delta G = -RT \ln K_x \quad (3)$$

RESULTS

Fluorescence of TMX-3 in Buffer. Tryptophan emission of TMX-3 was measured as a function of pH and peptide concentration, as summarized in Figure 2. At pH 5.3, at which the His residues were expected to be charged, the emission spectra were red-shifted and independent of peptide concentration (Figure 2A, arrow 1). For peptide concentrations of >10 μM, the spectra shifted toward blue wavelengths and higher quantum yields as the pH was increased, as expected for aggregation [Figure 2 (●)]. Fits of the data to Boltzmann curves yielded an apparent pK_a of 6.8 for His protonation (Figure 2B). Importantly, even at pH 7.6, the aggregation could be reversed by dilution of the peptide to a concentration of ≤10 μM (Figure 2A, arrow 2). This was not the case for the TMX-1 peptide (*16*), which exhibited a blue-shifted spectrum even at extremely low peptide concentrations (Figure 2A).

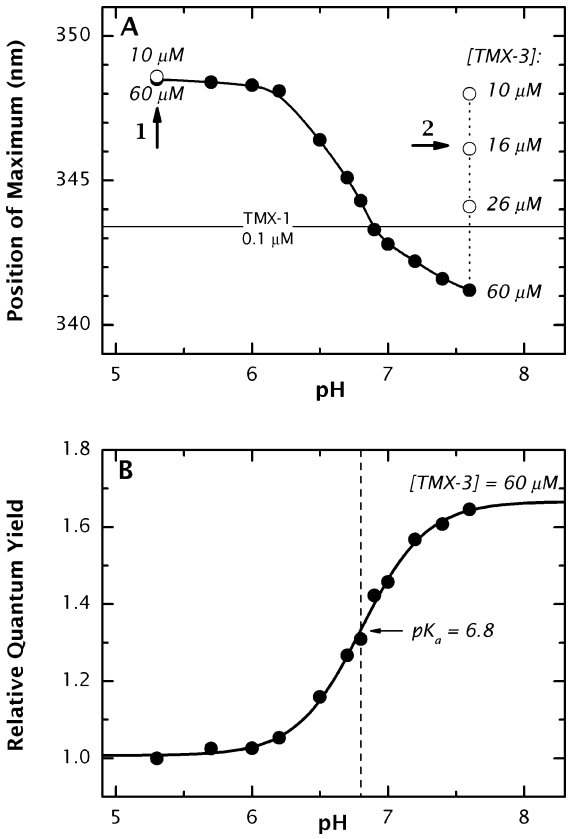

FIGURE 2: Fluorescence characteristics of TMX-3 in aqueous solution. pH dependence (A) of the position of maximal fluorescence emission and (B) of the relative quantum yield of TMX-3 in solution. At low pH, for which histidines are charged, the position of the maximum is red-shifted and independent of concentration (arrow 1). A concentrated sample (filled symbols) undergoes a monomer−aggregate transition as the pH increases. This results in a blue shift (A) and an increase in emission (B). The latter data can be fitted to a titration curve (solid line in panel B) with an apparent pK_a of 6.8 for His protonation. Even at high pH, the aggregation can be reversed by diluting the sample (panel A, empty symbols; arrow 2). At a concentration of 10 μM, TMX-3 has a red-shifted emission spectrum, consistent with the formation of the monomer at both high and low pH (see also Figure 3). This is different from TMX-1 (*16*), which exhibits a blue-shifted spectrum even at the lowest measurable concentration of 0.1 μM (horizontal line in panel B).

The conformational heterogeneity of TMX-3 was examined by means of position-width analysis (Figure 3) using the spectral parameters of fluorescence emission obtained from fits to eq 3 (*10*, *31*). Position-width analysis is based on the existence of discreet spectroscopic classes of tryptophan residues suggested by Burstein and co-workers (*31*) (named A, S, and I−III) (*32*−*34*) that are associated with defined combinations of spectral maxima and widths. These classes are related by a linear curve in plots of Γ versus λ_{max} (Figure 3). Trp residues in heterogeneous environments fall

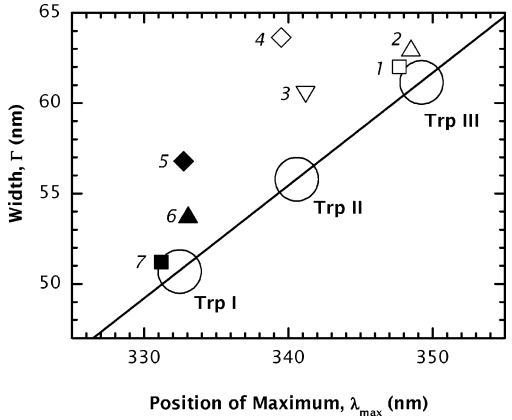

FIGURE 3: Position-width analysis of tryptophan fluorescence. The spectral parameters λ_{max} and Γ were obtained from log-normal fits according to eq 1 (see the text). The straight line is a reference line obtained from model studies (*10*). The large circles labeled Trp I−Trp III denote classes of Trp residues that correlate with the extent of water exposure according to Burstein et al. (*31*). The numbered, empty symbols are the data for peptides in solution: (1) TMX-3 monomer (10 μM) at pH 7.6, (2) TMX-3 monomer (10 μM) at pH 5.3, (3) TMX-3 aggregate (60 μM) at pH 5.3, and (4) TMX-1 aggregate (10 μM). The numbered filled symbols are the data for peptides in the presence of 1 mM POPC LUV: (5) TMX-1, (6) TMX-3 at pH 5.3, and (7) TMX-3 at pH 7.6. Data points 1, 4, 5, and 7 are from ref *10*. Aggregated samples exhibit considerable broadening, because they contain tryptophans of different spectral classes. Membrane-bound TMX-3 (point 7) has a spectrally homogeneous class I tryptophan. Although the position of the λ_{max} for membrane-bound TMX-1 (point 5) is similar, the spectral broadening observed for TMX-1 indicates conformational heterogeneity (see the text for details).

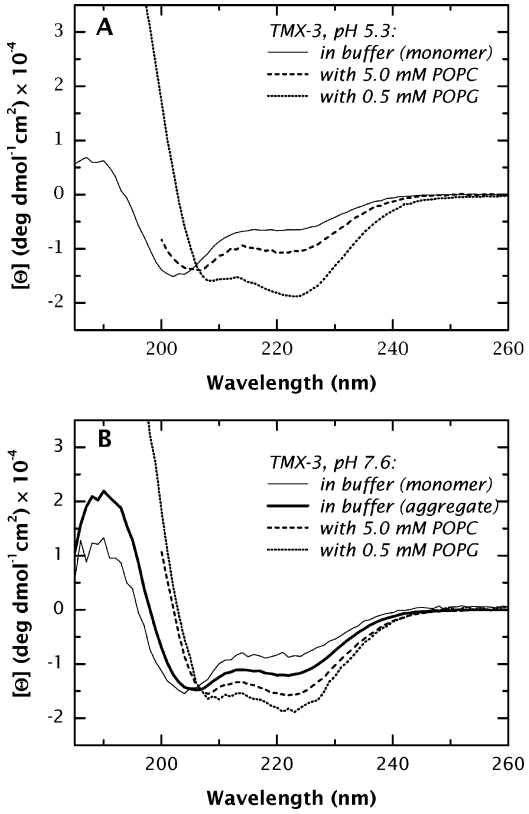

FIGURE 4: CD spectra of TMX-3 in buffer and in the presence of membranes at (A) pH 5.3 and (B) pH 7.6. The spectra of the monomeric peptide (thin solid lines) coincide at both pH values, indicating a predominantly unordered conformation with ~25% helical conformation. The aggregated form, which exists at only high pH, has a helicity of 40% (panel B, thick solid line). Binding to neutral POPC LUV (dashed lines) and anionic POPG LUV (dotted lines) results in increasing helicity. The exact helicity in POPC is difficult to estimate because it must be measured using very high lipid concentrations to saturate binding, especially at pH 5.3. The spectra in POPG, however, could be collected under saturating conditions. They indicate a helicity of approximately 70% for the membrane-bound peptide at either pH.

above the line as a result of being a mixture of classes. Using this approach, the position width of TMX-3 at low pH falls close to class III (points 1 and 2, Figure 3), meaning that Trp is in a nearly uniform environment with full water exposure. This is consistent with TMX-3 being monomeric at low pH. At elevated pH values and high concentrations, on the other hand, the position-width value of TMX-3 falls well above the linear curve (point 3). This is a hallmark of conformational heterogeneity with varying degrees of water exposure, as expected for aggregation. However, the degree of heterogeneity in TMX-3 is still far lower than that observed for TMX-1 (point 4, Figure 3), suggesting perhaps smaller aggregates. Regardless of the exact nature of the aggregated state, the important feature of TMX-3 is that its aggregation can be reversed by dilution, regardless of the protonation state of the His residues.

CD and OCD Measurements of TMX-3. CD spectra of TMX-3 in buffer (Figure 4) followed the same pattern as the fluorescence data (above). The spectra were independent of concentration at pH 5.3, but not at pH 7.6. At low concentrations, however, the spectra at pH 7.6 were found to be identical to those at pH 5.3. We attribute these spectra to the monomeric peptide (Figure 4). They indicate a predominantly unordered conformation with a helix content of ~25%. The aggregated high-pH form has a helicity of ~40% (thick solid line, Figure 4). Binding to neutral POPC LUV (- - -) and anionic POPG LUV (•••) results in increased helicity. The exact helicity of TMX-3 in POPC was difficult to estimate because it required making measurements under very high lipid concentrations to saturate the binding, especially at pH 5.3. Spectra in POPG, however, could be collected under saturating binding conditions. These indicated approximately 70% helicity of membrane-bound peptide at either pH, which corresponds to ~19−22 residues in a helical conformation.

The feasibility of TMX-3 adopting a transbilayer configuration was tested by performing oriented CD measurements on peptide-containing hydrated and oriented lipid multilayers. Samples were prepared by evaporation of an organic solvent containing a POPC and TMX-3 mixture (lipid-to-peptide ratio of 200). The OCD spectrum of TMX-3, recorded with the plane of the sample perpendicular to the beam, was typical (Figure 5) of an α-helix oriented parallel to the beam, i.e., normal to the membrane plane (*23*−*25*). A similar spectrum was observed for TMX-1 (*16*). Thus, both TMX-1 and TMX-3 adopt a predominantly transbilayer orientation in hydrated lipid multilayers after being cosolubilized with lipid in organic solvents. This shows that the insertion of TMX-3 across the LUV bilayer is thermodynamically feasible.

Fluorescence Changes Accompanying Partitioning of TMX-3 into Vesicles. The partitioning of TMX-3 into membranes, as for many other Trp-containing membrane peptides, caused an increase in fluorescence intensity and a

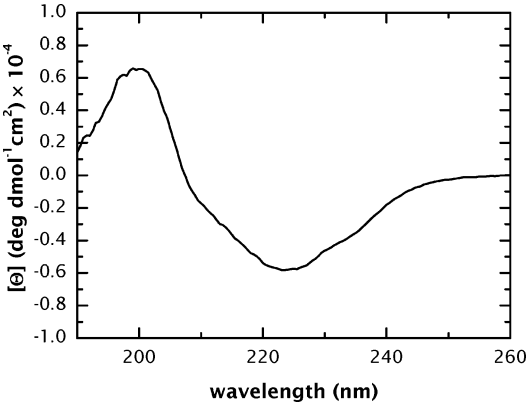

FIGURE 5: Oriented CD spectrum of TMX-3 in hydrated POPC multilayers deposited on a quartz slide oriented perpendicular to the beam. The lipid-to-peptide ratio was 200. The spectrum is consistent with the transbilayer orientation of the peptide under such conditions.

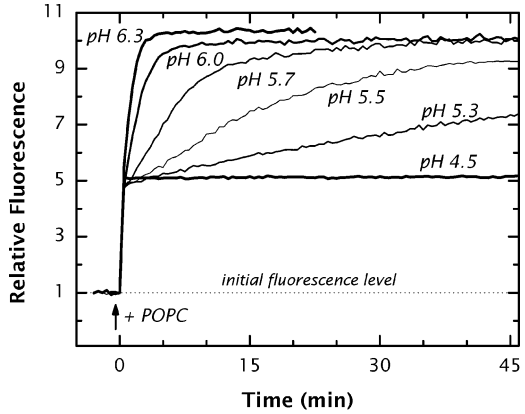

FIGURE 6: Kinetics of fluorescence increase upon binding of TMX-3 to POPC LUV. Membrane binding results in an increase in fluorescence intensity that follows a complex kinetic pattern. First, the intensity increases rapidly to an intermediate level, which is largely pH-independent. For a sample at pH 4.5, the intensity remains at this level, while for samples at higher pHs, the intensity increases further. The rate of this second step depends on the pH and ranges from hours (pH 5.3) to minutes (pH 6.3).

blue shift of the emission spectrum. The kinetics-of-fluorescence increase, however, followed a peculiar two-step pattern that we have not previously observed (Figure 6). First, the intensity increased rapidly to an intermediate level that was mainly pH-independent. The intensity remained at this level for samples at pH 4.5, while for samples at higher pHs, the intensity increased further. The rate of this second step depended on the pH and ranged from hours (pH 5.3) to minutes (pH 6.3). Note that all the curves in Figure 6 were for pH values well below 6.8 (pH = pK_a), meaning that titration of the TMX-3 His residues in solution had not begun (Figure 2). The pH-dependent behavior of the membrane binding kinetics should thus depend on only the protonation state of the TMX-3 His residues in the membrane environment (see Discussion). At higher pH values, for which aqueous TMX-3 His residues were deprotonated, the intensity increased in one step to the high level (not shown, but similar to that at pH 6.3). The kinetics of the increase were apparently very fast within the time resolution that could be obtained with hand mixing.

We also evaluated the conformational heterogeneity of membrane-bound TMX-3 by position-width analysis of Trp

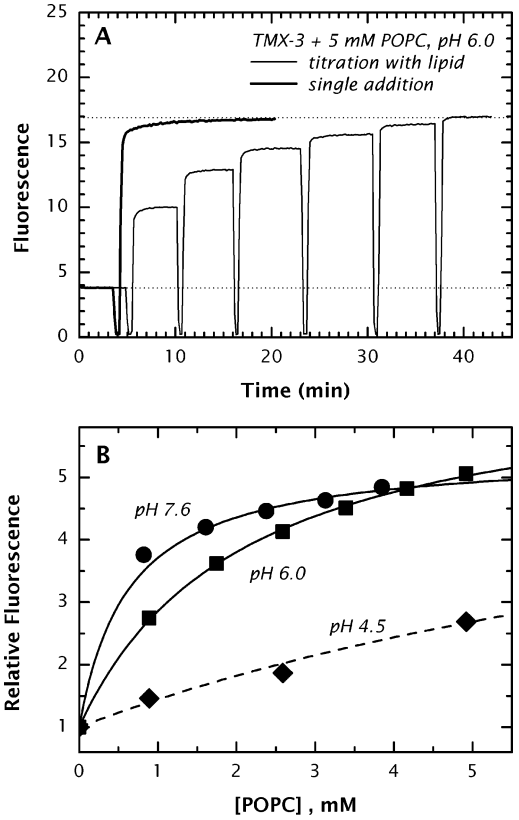

FIGURE 7: Determination of the free energy of membrane partitioning of TMX-3 by fluorescence titration. (A) Titration of a TMX-3 solution with POPC LUV. POPC LUV (5 mM) were added to two identical samples of TMX-3, either in one addition (thick line) or in six increments (thin line). In both cases, the total intensity increase was the same, indicating that the final state was independent of the history of the sample. (B) Titration data (symbols), from experiments such as those in panel A used for free energy determinations. Solid lines are best fits of data to eq 2, which yield the following values of ΔG: −6.7 kcal/mol at pH 7.6 (●), −6.0 kcal/mol at pH 6.0 (■), and approximately −5 kcal/mol at pH 4.5 (◆). In the latter fit, the parameter of maximum intensity increase was kept constant (see the text for details).

fluorescence (filled symbols in Figure 3). The Trp of TMX-3 in POPC LUV at pH 7.6 (Figure 3, point 7) had a spectrum of a pure class I Trp. This is consistent with the IF location of the fluorophore, because it is also observed for other interface-binding peptides, e.g., melittin (*10*). The spectrum was broadened somewhat at pH 5.3 (Figure 3, point 6), which is likely due to incomplete binding under these conditions. This is different from TMX-1 (*10*). Even under conditions of practically complete binding, TMX-1 exhibited extra broadening (Figure 3, point 5) that is consistent with conformational heterogeneity.

Energetics of Partitioning of TMX-3 into POPC LUV. Increases in fluorescence upon membrane association can be used to determine the free energy of membrane partitioning in titration experiments, provided that the system remains at equilibrium. A hallmark of a system at equilibrium is that the final state is independent of the path by which it is reached. We therefore tested the membrane partitioning of TMX-3 for equilibrium by comparing the results of two different titrations. POPC LUV (5 mM) were added to two identical samples of TMX-3 (Figure 7A), either in one addition (thick line) or in six increments (thin line; during the addition of vesicles, the shutters were closed, causing

the intensity to drop to zero). The initial and final intensities in both cases were the same (dotted lines), indicating that the final state was independent of the history of the sample.

To determine partition coefficients, we measured the increases in fluorescence intensity of TMX-3 upon titration with POPC LUV at pH 4.5, 6.0, and 7.6 (Figure 7B, symbols) and fitted eq 2 to the data (Figure 7B, curves). The best-fit values of the mole-fraction partition coefficient (K_x) and the fluorescence increase upon complete binding (I_∞) were as follows: $K_x = (8.8 \pm 3.0) \times 10^4$ and $I_\infty = 5.4 \pm 0.1$ for pH 7.6, $K_x = (2.7 \pm 0.4) \times 10^4$ and $I_\infty = 6.7 \pm 0.1$ for pH 6.0, and $K_x = (5.0 \pm 1.5) \times 10^3$ and I_∞ fixed at 6.7 for pH 4.5. Because binding at pH 4.5 was very weak and far from saturation even at 5 mM LUV, it was necessary to restrict the fitting parameters at this pH to obtain a reasonable estimate of partitioning. Fixing I_∞ at any value between 5 and 8 yielded practically the same value of K_x. The dashed line in Figure 7B corresponds to the fit for which I_∞ was set equal to 6.7 (best-fit value at pH 6.0). The free energies of transfer (ΔG) of TMX-3 from water to membrane (eq 3) were found to be -6.7 ± 0.3 kcal/mol at pH 7.6, -6.0 ± 0.1 kcal/mol at pH 6.0, and approximately -5 kcal/mol at pH 4.5.

Topology of TMX-3. The topology of TMX-3 in lipid vesicles was determined using the LysoMC quenching method (*26*), which allows one to determine if a Trp residue is located in the outer or inner leaflet of the membrane. Because the C-terminus is highly charged, it was not expected to translocate across the membrane. Therefore, if the Trp (located at the N-terminus) is found in the outer leaflet, the peptide is bound interfacially, while if the Trp is found in the inner leaflet, the peptide must be in a transbilayer orientation.

The LysoMC quenching experiments were carried out as described in Materials and Methods. A three-step procedure was used, during which the Trp spectrum was measured in the presence of the following distributions of quenchers: (1) 0.5% asymmetric LysoMC (all in *cis* leaflet), (2) 1.0% asymmetric LysoMC (all in *cis* leaflet), and (3) 1.0% symmetric LysoMC (half in *cis* and half in *trans* leaflet). The curves in Figure 8 are numbered according to these steps. The un-numbered curves, corresponding to vesicle-bound TMX-3 in the absence of LysoMC, are given for reference, but were not used for determination of the Trp topology. The peaks at 400 nm, resulting from direct excitation of LysoMC, are also shown for visual reference. The information about topology (defined as a *cis* or *trans* location) of Trp is contained in the relative intensities of curves 1−3 in the region of Trp emission (300−350 nm). According to the single-sample experimental scheme used here, the following hallmarks were considered for the interpretation of the experimental data (*29*). (a) Curve 3 has a higher intensity than curve 2 when the Trp probe is located predominantly on the *cis* side. (Note that curves 3 and 1 coincide when the probe is exclusively on the *cis* side.) (b) Curves 2 and 3 coincide when the probe is equally distributed between the *cis* and *trans* sides. (c) Curve 3 has the lowest intensity when the probe is predominantly on the *trans* side.

As shown in Figure 8, the TMX-3 Trp is in the outer leaflet at low peptide concentrations (curves 1 and 3 coincide, Figure 8A) and is partially translocated at higher concentrations (curve 3 is between curves 1 and 2, Figure 8B). The

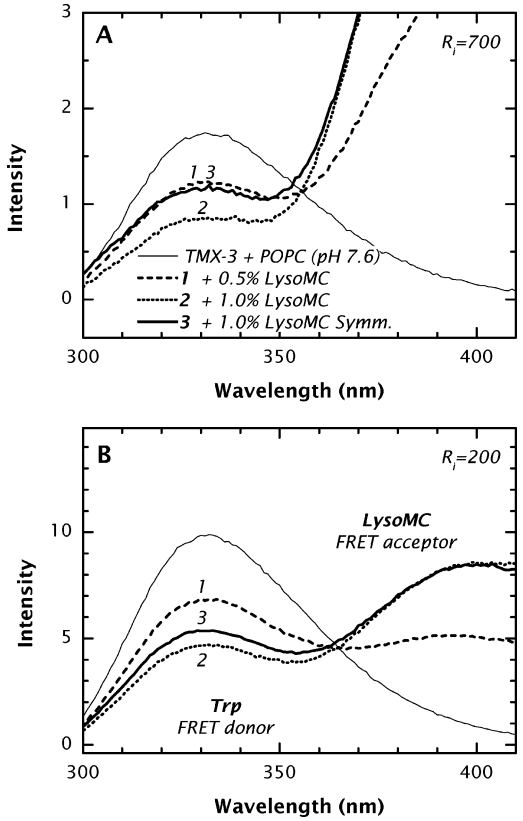

FIGURE 8: Determination of the peptide topology at two peptide concentrations using LysoMC as a FRET quencher of Trp fluorescence at (A) a low peptide concentration ($R_i = 700$) and (B) a high peptide concentration ($R_i = 200$). The original two-sample assay of Wimley and White (*26*) was modified to make it a single-sample experimental scheme (*29*), described in Materials and Methods. The unlabeled curves in each panel represent the Trp fluorescence of TMX-3 bound to 4 mM POPC LUV at pH 7.6 in the absence of quenching after a 4 h preincubation. The numbers of the curves correspond with the following distributions of LysoMC: (1) 0.5% asymmetric (outer leaflet) LysoUB, (2) 1.0% asymmetric (outer leaflet) LysoUB, and (3) 1.0% symmetric (both leaflets) LysoUB. At low concentrations, the increase in the intensity of curve 3 in panel A to the level of curve 1 indicates that the Trp residue has not been translocated and that the peptide adopts an interfacial topology. At high concentrations, the position of curve 3 in panel B between curves 1 and 2 indicates partial transbilayer insertion of the peptide (see the text for details).

degree of Trp translocation is ∼30−40%, which is similar to the value of ∼50% reported for TMX-1 (*16*). The titration data depicted in Figure 7 were collected in the low-concentration regime, for which TMX-3 binds within the IF region without crossing the bilayer. An important question was whether equilibrium membrane association could occur at the high concentrations that cause TMX-3 to insert across the bilayer.

To determine if insertion of TMX-3 in a transbilayer conformation was reversible, we conducted a membrane exchangeability experiment (*16*) (Figure 9). We first measured Trp emission in 3 mM POPC vesicles and in vesicles formed from the fluorescence-quenching lipid OBPC. In both cases, a high lipid-to-peptide ratio ($R_i = 200$) was used to encourage the insertion. Fluorescence was measured after the samples had been incubated for 4 h at 25 °C to ensure equilibration. The POPC sample (curve 1) had a high intensity, while the OBPC sample (curve 2) had a low intensity due to quenching with bromine atoms. Next, 3 mM

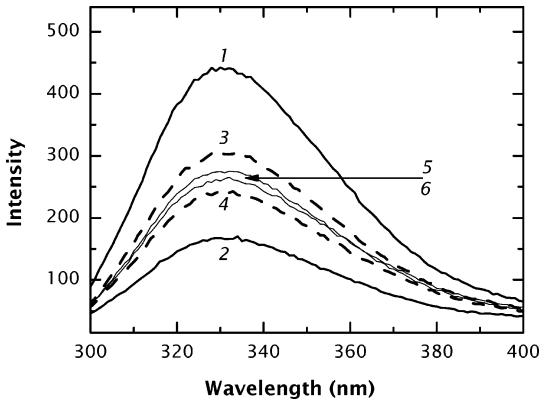

FIGURE 9: Test of the reversibility of transmembrane insertion of TMX-3 into zwitterionic LUV. In these experiments, we first measured Trp emission in 3 mM POPC vesicles (curve 1) and in vesicles formed from the fluorescence-quenching lipid OBPC (curve 2). In both cases, a high lipid-to-peptide ratio ($R_i = 200$) was used to encourage insertion. After incubation for 4 h, an amount of OBPC was added to the POPC sample (curve 3) that equaled an amount of POPC added to the OBPC sample. The fluorescence signals of the samples were determined after incubation for an additional 12 h (curves 3 and 4, POPC-to-OBPC and OBPC-to-POPC exchange, respectively). In the case of complete exchange, curves 3 and 4 would have been identical. That they were not identical indicates hindered reversibility of insertion. Complete reversibility was achieved, however, after both samples were heated to 60 °C for 40 min and then brought back to 25 °C (curves 5 and 6).

POPC LUV were added to the OBPC sample and 3 mM OBPC was added to the POPC sample. Following incubation for an additional 12 h, the intensity of the original POPC sample had dropped (curve 3) while that of the original OBPC sample had increased (curve 4), indicating substantial, but not complete, exchange of peptides among the vesicles. Had the exchange been complete, curves 3 and 4 would have been identical. That they were not identical indicates hindered reversibility of insertion. To ensure that complete reversibility was possible given a sufficiently long equilibration period, both samples were heated to 60 °C for 40 min and then brought back to 25 °C (curves 5 and 6). Practically complete reversibility could be achieved under these circumstances.

DISCUSSION

The rationale for designing the TMX peptides is the development of model peptides for studying the refolding and insertion of nonconstitutive membrane proteins, such as diphtheria toxin. Our first peptide in the series (*16*), TMX-1, revealed that the principal difficulty in designing spontaneously inserting TM peptides is aggregation in the aqueous phase. The data presented here show that the design features incorporated into TMX-3 have overcome this problem. The key features that ensure a monomeric state over a useful concentration range are those that discourage excessive helix formation in solution, namely, elimination of helical caps and alanine heptad repeats and the introduction of a proline and two histidines into the presumed TM domain. These features cause TMX-3 to exist as an unordered monomer over a wide pH range at a concentration of 10 μM (Figure 2). At pH values below the His pK_a of 6.8, TMX-3 remains monomeric at concentrations as high as 60 μM (Figure 2A). These features do not prevent TMX-3 from binding reversibly to neutral membranes (Figure 6). The position-width fluorescence analysis of TMX-3 shows that its Trp residue exists in a spectroscopically homogeneous environment at the membrane interface. This is different from that with TMX-1, whose substantial spectral broadening suggests large multimeric aggregates in both the aqueous and membrane environments.

There are two regimes of TMX-3 membrane interactions. At low concentrations, it adopts an IF topology, while at higher concentrations, it begins to insert across the bilayer (Figure 8). The insertion efficiency is not high; only approximately one-third of the peptide is in the transbilayer conformation at a lipid-to-peptide ratio of 200. Insertion at higher concentrations could not be explored because the peptide caused lipid flip-flop, which interfered with the topology assay (data not shown). A similar degree of insertion was also observed with TMX-1, for which the LysoMC topology method suggested that approximately half of the Trp residues were translocated (*16*). Spontaneous insertion of a helix into a preformed LUV bilayer requires crossing an energy barrier separating the IF and TM conformations. The existence of a substantial barrier was confirmed by the exchange experiments (Figure 9). The concentration dependence of insertion can arise either from lowering the energy barrier via collective perturbation of the bilayer, perhaps by an accumulation of the IF form, or from the formation of specific peptide aggregates.

The mode of membrane interaction of TMX-3 clearly indicates the importance of the IF conformation. In fact, at low concentrations, the peptide is a good template for host−guest free energy measurements of IF partitioning. The Wimley−White (W−W) IF hydrophobicity scale was determined experimentally by using an unfolded pentapeptide template (*12*). The accuracy of the W−W IF scale has been demonstrated using a larger, but still unfolded, template based upon the 13-residue antimicrobial peptide indolicidin (*15*). To be able to predict partitioning of polypeptides that form a hydrogen-bonded secondary structure on membrane interfaces, two issues need to be considered. First, the contribution of the folding free energy of −0.1 to −0.5 kcal/mol per residue needs to be taken into account (*13*, *14*, *35*, *36*). Second, the W−W IF scale needs to be tested in the context of an interfacial helical template. TMX-3 is an ideal candidate for such a study.

The first test of the applicability of the Wimley−White IF scale for relative prediction of interfacial binding of helical peptides comes from the pH dependence of the free energy of transfer of TMX-3 (Figure 7). As illustrated by the thermodynamic cycles in Figure 10A, the two His residues are charged at pH 4.5 in both the water-soluble (I_c) and membrane-bound forms (III_c). Partitioning of charged residues into the interface is unfavorable, and hence, the favorable free energy is relatively low. At pH 7.6, the His residues of TMX-3 in both the bound (III_n) and free peptide (I_n) are deprotonated, resulting in an increase in the favorable free energy. The ΔG between the charged and neutral states estimated from our data is −0.85 kcal/mol per His. This is close to the value of −0.79 kcal/mol expected from the W−W IF hydrophobicity scale (*12*). At the intermediate pH of 6.0, the peptide in solution still has protonated histidines (pK_a = 6.8; Figure 2), but on the membrane His, deprotonation occurs due to a lowered pK_a value. This leads to the appearance of form III_n, which has a higher affinity for the membrane than form III_c. Form III_n accumulates until it

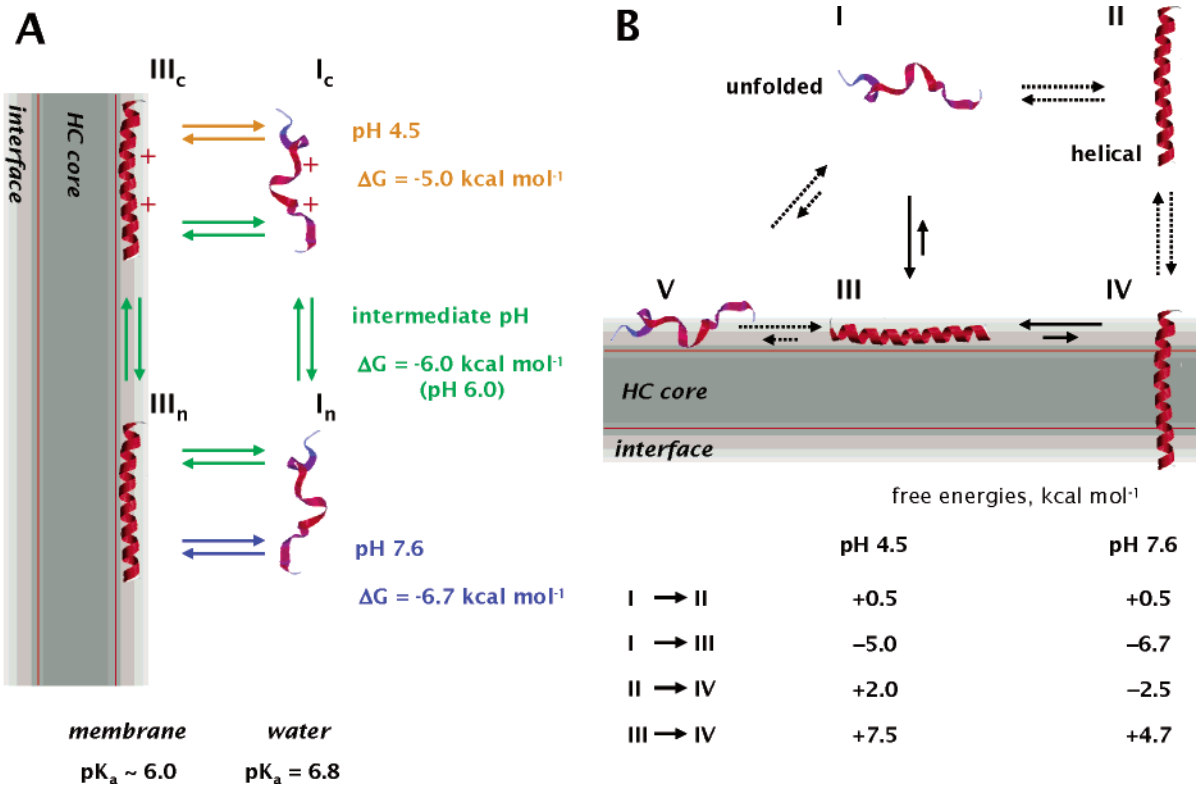

FIGURE 10: Thermodynamic cycles for membrane partitioning of TMX-3 at different pH values. (A) Thermodynamic cycles for interfacial membrane partitioning of TMX-3 using the nomenclature of panel B. At pH 4.5, the two His residues are charged (indicated with +) in both the water-soluble (I_c) and membrane-bound forms (III_c). Partitioning of charged residues into the interface is unfavorable, and hence, the favorable free energy is lower. At pH 7.6, the histidines in both the bound (III_n) and free peptide (I_n) are neutral (deprotonated), resulting in a free energy increase. Remarkably, the difference of −0.85 kcal/mol per histidine estimated from our data corresponds closely to the value of −0.79 kcal/mol in the free energy of partitioning computed using the Wimley−White interfacial hydrophobicity scale (*12*) (see the text). At the intermediate pH of 6.0, the peptide in solution still has protonated histidines ($pK_a = 6.8$; Figure 2). On the membrane, however, histidine deprotonation occurs, due to a lower value of pK_a. This leads to the appearance of form III_n, which has a higher affinity for the membrane than form III_c. Form III_n accumulates until it reaches equilibrium with the I_n form, which is quickly converted back to I_c. This interfacial deprotonation and subsequent re-equilibration is responsible for the biphasic kinetics of binding (Figure 6) and the additional gain in free energy as compared to that at pH 4.5. (B) Summary of membrane interactions of TMX-3. The numbers beneath the figure correspond to the transfer free energy values (in kilocalories per mole) estimated experimentally or computationally in this study (see the text for details). Regardless of the pH-dependent protonation state of histidines in TMX-3, the interfacial folded state is the most energetically favorable state. The dashed arrows show pathways in the thermodynamic cycle that are not accessible experimentally.

reaches equilibrium with form I_n, which is quickly converted back to I_c. This interfacial deprotonation and subsequent re-equilibration explains the slow component in the biphasic kinetics of binding (Figure 6), and the additional gain in free energy as compared to that at pH 4.5. At pH 6.0, the ΔG value is approximately halfway between the values at pH 7.6 and 4.5 (Figures 7 and 10). This suggests that the $pK_a \approx 6$ on the membrane interface.

The energy of protonation of titratable residues is known to depend on the dielectric properties of their environment (*37*). Bechinger (*20*) observed a pK_a change of 1.7 units for His residues in a detergent micelle environment. Fernandez and Fromherz (*38*) reported a 1.0−1.5 pH unit difference in pK_a between dyes in water and neutral micelle detergents. Wimley et al. (*39*) observed that the carboxy terminus of pentapeptides had a pK_a of 3.7 in buffer and 7.0 in wet octanol. Thus, it is not surprising that partitioning into a lipid bilayer would have a similar effect on the His pK_a. It is significant, however, that His deprotonation of TMX-3 occurs in the interfacial region of the bilayer. This may have important implications for the pH-triggered insertion of many proteins, such as diphtheria toxin (*1*), colicin E1 (*4*), and annexin 12 (*8*, *29*). All of these proteins insert at low pH, at which histidines are generally assumed to be charged. Our results suggest that partitioning into the bilayer interface may result in the deprotonation of histidines. This may "stage" the proteins for further transmembrane insertion due to protonation of Glu and Asp residues.

The concentration dependence of TMX-3 insertion may also be related to the insertion pathway of toxins and other spontaneously inserting proteins. To enter the membrane, they must pass through the interfacial region of the bilayer. Our data suggest that transbilayer insertion begins only after the concentration of interfacial helices is sufficiently high, perhaps, to stress the membrane. One can thus speculate that an important step in the interfacial refolding of a nonconstitutive protein in the interfacial region of the bilayer is the formation of an intermediate with a high local interfacial concentration that "stresses" the bilayer as a prelude to further insertion.

Our results can be summarized by means of the thermodynamic cycle of Figure 10B, which considers five states: unfolded in water (I), helical in water (II), helical on the membrane interface (III), transmembrane helical (IV), and unfolded on the membrane interface (V). The experimental measurements reported here in conjunction with theoretical

estimates allow reasonable values of the free energy differences among the states to be estimated. The W−W experiment-based whole-residue hydrophobicity scales (*12*, *40*, *41*) provide useful estimates of the energetics of TMX-3 folding along this thermodynamic cycle. For the 20-residue hydrophobic core (residues 3−22) of TMX-3 transferred as an α-helix from water to the bilayer (II−IV transition, Figure 10B), $\Delta G = 2.0$ and −2.5 kcal/mol, for charged and neutral histidines, respectively. Although these numbers indicate that deprotonation of histidines leads to favorable insertion of an α-helix, the story is incomplete because the IF state must be taken into account. The W−W IF hydrophobicity scale (*12*), combined with the estimated free energy reduction of −0.4 kcal/mol per residue involved in helix formation determined by Ladokhin and White (*13*), predicts the free energy of the transfer of the unordered conformation in water (I) to an interfacial helical conformation (III) ranges from −4.5 to −8.4 kcal/mol for charged histidines and from −6.0 to −10.0 kcal/mol for neutral ones. The exact values depend on whether the entire peptide or only the hydrophobic span penetrates the interface. The experimentally determined values for the I−III transition, −5.0 and −6.7 kcal/mol, fall comfortably within these predicted ranges.

TMX-3 in the monomeric state is only partially helical (∼25%) in the aqueous phase, but readily gains helicity upon interaction with membranes (Figure 4). This makes it very similar to melittin, for which the coil−helix free energy transition in water is unfavorable (*42*), especially compared with the large favorable folding free energy on the membrane interface (*13*). One can thus reasonably assume for TMX-3 that the ΔG for the I−II transition is slightly positive (*42*). Given ∼25% helicity, we estimate that $\Delta G \approx 0.5$ kcal/mol, but the exact value does not affect our principal conclusions.

With the above considerations, the folded IF helix−TM helix transition (III−IV) can be estimated (Figure 10B). The results suggest that the TM orientation is not preferred over the interfacial one, even at high pH for which the histidines are neutral. The difference of 4.7 kcal/mol is equivalent to approximately one molecule in the TM state for every 3000 in the IF state. This is consistent with the experimentally observed lack of translocation in the low-concentration regime of TMX-3 membrane penetration (Figure 8A). In the high-concentration regime, ∼30% of the molecules are translocated (Figure 8B), which translates into a ΔG value of ∼0.4 kcal/mol. The difference between insertion at low and high peptide-to-lipid ratios can be explained either by a lowering of the free energy of insertion during membrane aggregation or by collective perturbation of the bilayer by the peptide. Highly aggregated TMX-1 inserts with an efficiency of 50% (*16*); i.e., the free energy for the IF helix−TM helix transition is approximately zero. Alternatively, the concentration dependence of insertion may involve collective perturbation of the bilayer, as demonstrated for peptide antibiotics (*43*−*45*). It is quite difficult to distinguish between these two explanations experimentally. In any case, our results indicate that interfacial conformations can be energetically very favorable for peptides such as TMX-3, and presumably more complex proteins such as diphtheria toxin T-domain. An important question is just how hydrophobic a TMX peptide would have to be for the TM configuration to be strongly favored. From the W−W hydrophobicity scales, we estimate that seven Ala-to-Leu substitutions in TMX-3 would be required for an IF:TM ratio of 1:60, corresponding to an IF helix−TM helix ΔG of −2.4 kcal/mol.

ACKNOWLEDGMENT

We thank Michael Myers for his editorial assistance.

REFERENCES

1. Oh, K. J., Senzel, L., Collier, R. J., and Finkelstein, A. (1999) Translocation of the catalytic domain of diphtheria toxin across planar phospholipid bilayers by its own T domain, *Proc. Natl. Acad. Sci. U.S.A. 96*, 8467−8470.
2. Miller, C. J., Elliott, J. L., and Collier, R. J. (1999) Anthrax protective antigen: Prepore-to-pore conversion, *Biochemistry 38*, 10432−10441.
3. Shatursky, O., Heuck, A. P., Shepard, L. A., Rossjohn, J., Parker, M. W., Johnson, A. E., and Tweten, R. K. (1999) The mechanism of membrane insertion for a cholesterol-dependent cytolysin: A novel paradigm for pore-forming toxins, *Cell 99*, 293−299.
4. Zakharov, S. D., Lindberg, M., Griko, Y., Salamon, Z., Tollin, G., Prendergast, F. G., and Cramer, W. A. (1998) Membrane-bound state of the colicin E1 channel domain as an extended two-dimensional helical array, *Proc. Natl. Acad. Sci. U.S.A. 95*, 4282−4287.
5. Zakharov, S. D., Lindeberg, M., and Cramer, W. A. (1999) Kinetic description of structural changes linked to membrane import of the colicin E1 channel protein, *Biochemistry 38*, 11325−11332.
6. Parker, M. W., Tucker, A. D., Tsernoglou, D., and Pattus, F. (1990) Insights into membrane insertion based on studies of colicins, *Trends Biochem. Sci. 15*, 126−129.
7. Gerber, D., and Shai, Y. (2002) Chirality-independent protein−protein recognition between transmembrane domains in vivo, *J. Mol. Biol. 322*, 491−495.
8. Langen, R., Isas, J. M., Hubbell, W. L., and Haigler, H. T. (1998) A transmembrane form of annexin XII detected by site-directed spin labeling, *Proc. Natl. Acad. Sci. U.S.A. 95*, 14060−14065.
9. Isas, J. M., Cartailler, J.-P., Sokolov, Y., Patel, D. R., Langen, R., Luecke, H., Hall, J. E., and Haigler, H. T. (2000) Annexins V and XII insert into bilayers at mildly acidic pH and form ion channels, *Biochemistry 39*, 3015−3022.
10. Ladokhin, A. S., Jayasinghe, S., and White, S. H. (2000) How to measure and analyze tryptophan fluorescence in membranes properly, and why bother? *Anal. Biochem. 285*, 235−245.
11. White, S. H., Ladokhin, A. S., Jayasinghe, S., and Hristova, K. (2001) How membranes shape protein structure, *J. Biol. Chem. 276*, 32395−32398.
12. Wimley, W. C., and White, S. H. (1996) Experimentally determined hydrophobicity scale for proteins at membrane interfaces, *Nat. Struct. Biol. 3*, 842−848.
13. Ladokhin, A. S., and White, S. H. (1999) Folding of amphipathic α-helices on membranes: Energetics of helix formation by melittin, *J. Mol. Biol. 285*, 1363−1369.
14. Wimley, W. C., Hristova, K., Ladokhin, A. S., Silvestro, L., Axelsen, P. H., and White, S. H. (1998) Folding of β-sheet membrane proteins: A hydrophobic hexapeptide model, *J. Mol. Biol. 277*, 1091−1110.
15. Ladokhin, A. S., and White, S. H. (2001) Protein chemistry at membrane interfaces: Non-additivity of electrostatic and hydrophobic interactions, *J. Mol. Biol. 309*, 543−552.
16. Wimley, W. C., and White, S. H. (2000) Designing transmembrane α-helices that insert spontaneously, *Biochemistry 39*, 4432−4442.
17. Gernert, K. M., Surles, M. C., Labean, T. H., Richardson, J. S., and Richardson, D. C. (1995) The Alacoil: A very tight, antiparallel coiled-coil of helices, *Protein Sci. 4*, 2252−2260.
18. Presta, L. G., and Rose, G. D. (1988) Helix signals in proteins, *Science 240*, 1632−1641.
19. Richardson, J. S., and Richardson, D. C. (1988) Amino Acid Preferences for Specific Locations at the Ends of α Helices, *Science 240*, 1648−1652.
20. Bechinger, B. (1996) Towards membrane protein design: pH-sensitive topology of histidine-containing polypeptides, *J. Mol. Biol. 263*, 768−775.
21. Vogel, H., and Jähnig, F. (1986) The structure of melittin in membranes, *Biophys. J. 50*, 573−582.

22. Oren, Z., and Shai, Y. (1997) Selective lysis of bacteria but not mammalian cells by diastereomers of melittin: Structure−function study, *Biochemistry 36*, 1826−1835.
23. Olah, G. A., and Huang, H. W. (1988) Circular dichroism of oriented α helices. I. Proof of the exciton theory, *J. Chem. Phys. 89*, 2531−2538.
24. Olah, G. A., and Huang, H. W. (1988) Circular dichroism of oriented α helices. II. Electric field oriented polypeptides, *J. Chem. Phys. 89*, 6956−6962.
25. Wu, Y., Huang, H. W., and Olah, G. A. (1990) Method of oriented circular dichroism, *Biophys. J. 57*, 797−806.
26. Wimley, W. C., and White, S. H. (2000) Determining the membrane topology of peptides by fluorescence quenching, *Biochemistry 39*, 161−170.
27. Hope, M. J., Bally, M. B., Mayer, L. D., Janoff, A. S., and Cullis, P. R. (1986) Generation of multilamellar and unilamellar phospholipid vesicles, *Chem. Phys. Lipids 40*, 89−107.
28. Mayer, L. D., Hope, M. J., and Cullis, P. R. (1986) Vesicles of variable sizes produced by a rapid extrusion procedure, *Biochim. Biophys. Acta 858*, 161−168.
29. Ladokhin, A. S., Isas, J. M., Haigler, H. T., and White, S. H. (2002) Determining the membrane topology of proteins: Insertion pathway of a transmembrane helix of annexin 12, *Biochemistry 41*, 13617−13626.
30. White, S. H., Wimley, W. C., Ladokhin, A. S., and Hristova, K. (1998) Protein folding in membranes: Determining the energetics of peptide-bilayer interactions, *Methods Enzymol. 295*, 62−87.
31. Burstein, E. A., Vedenkina, N. S., and Ivkova, M. N. (1973) Fluorescence and the location of tryptophan residues in protein molecules, *Photochem. Photobiol. 18*, 263−279.
32. Burstein, E. A., Abornev, S. M., and Reshetnyak, Y. K. (2001) Decomposition of protein tryptophan fluorescence spectra into log-normal components. I. Decomposition algorithms, *Biophys. J. 81*, 1699−1709.
33. Reshetnyak, Y. K., and Burstein, E. A. (2001) Decomposition of protein tryptophan fluorescence spectra into log-normal components. II. The statistical proof of discreteness of tryptophan classes in proteins, *Biophys. J. 81*, 1710−1734.
34. Reshetnyak, Y. K., Koshevnik, Y., and Burstein, E. A. (2001) Decomposition of protein tryptophan fluorescence spectra into log-normal components. III. Correlation between fluorescence and microenvironment parameters of individual tryptophan residues, *Biophys. J. 81*, 1735−1758.
35. Wieprecht, T., Apostolov, O., Beyermann, M., and Seelig, J. (1999) Thermodynamics of the α-helix-coil transition of amphipathic peptides in a membrane environment: Implications for the peptide-membrane binding equilibrium, *J. Mol. Biol. 294*, 785−794.
36. Li, Y., Han, X., and Tamm, L. K. (2003) Thermodynamics of fusion peptide-membrane interactions, *Biochemistry 42*, 7245−7251.
37. Fitch, C. A., Karp, D. A., Lee, K. K., Stites, W. E., Lattman, E. E., and García-Moreno, E. B. (2002) Experimental pK_a values of buried residues: Analysis with continuum methods and role of water penetration, *Biophys. J. 82*, 3289−3304.
38. Fernandez, M. S., and Fromherz, P. (1977) Lipoid pH indicators as probes of electrical potential and polarity in micelles, *J. Phys. Chem. 81*, 1755−1761.
39. Wimley, W. C., Gawrisch, K., Creamer, T. P., and White, S. H. (1996) A direct measurement of salt-bridge solvation energies using a peptide model system: Implications for protein stability, *Proc. Natl. Acad. Sci. U.S.A. 93*, 2985−2990.
40. Wimley, W. C., Creamer, T. P., and White, S. H. (1996) Solvation energies of amino acid side chains and backbone in a family of host−guest pentapeptides, *Biochemistry 35*, 5109−5124.
41. White, S. H., and Wimley, W. C. (1999) Membrane protein folding and stability: Physical principles, *Annu. Rev. Biophys. Biomol. Struct. 28*, 319−365.
42. Hirota, N., Mizuno, K., and Goto, Y. (1998) Group additive contributions to the alcohol-induced α-helix formation of melittin: Implication for the mechanism of the alcohol effects on proteins, *J. Mol. Biol. 275*, 365−378.
43. Ludtke, S. J., He, K., Wu, Y. L., and Huang, H. W. (1994) Cooperative membrane insertion of magainin correlated with its cytolytic activity, *Biochim. Biophys. Acta 1190*, 181−184.
44. Huang, H. W. (2000) Action of antimicrobial peptides: Two-state model, *Biochemistry 39*, 8347−8352.
45. Chen, F.-Y., Lee, M.-T., and Huang, H. W. (2003) Evidence for membrane thinning effect as the mechanism for peptide-induced pore formation, *Biophys. J. 84*, 3751−3758.

BI0361259